Journal of Magnetism and Magnetic Materials 378 (2015) 41–49

Contents lists available at ScienceDirect

Journal of Magnetism and Magnetic Materials

journal homepage: www.elsevier.com/locate/jmmm

First-principles calculations of a half-metallic ferromagnet zinc blende $Zn_{1-x}V_xTe$

M. El Amine Monir [a], H. Baltache [a], R. Khenata [a,*], G. Murtaza [b], Sikander Azam [c], A. Bouhemadou [d], Y. Al-Douri [e], S. Bin Omran [f], Roshan Ali [g]

[a] Laboratoire de Physique Quantique de la Modélisation Mathématique (LPQ3M), Université de Mascara, 29000, Algeria
[b] Materials Modeling Laboratory, Department of Physics, Islamia College University, Peshawar, Pakistan
[c] New Technologies-Research Center, University of West Bohemia, Univerzitni 8, 306 14 Pilsen, Czech republic
[d] Laboratory for Developing New Materials and their Characterization, Department of Physics, Faculty of Science, University Setif 1, 19000 Setif, Algeria
[e] Institute of Nano Electronic Engineering, University Malaysia Perlis, 01000 Kangar, Perlis, Malaysia
[f] Department of Physics and Astronomy, College of Science, King Saud University, P.O. Box 2455, Riyadh 11451, Saudi Arabia
[g] Materials Modeling Lab, Department of Physics, Post Graduate Jahanzeb College, Swat, Pakistan

ARTICLE INFO

Article history:
Received 21 March 2014
Received in revised form
25 August 2014
Accepted 16 October 2014
Available online 7 November 2014

Keywords:
First-principles calculations
Half-metallic ferromagnetism
Electronic properties
Magnetic properties

ABSTRACT

First-principles calculations have been used to study the structural, elastic, electronic, magnetic and thermal properties of zinc blende $Zn_{1-x}V_xTe$ for $x=0$, 0.25, 0.50, 0.75 and 1 using the full-potential linearized augmented plane wave method (FP-LAPW) based on spin-polarized density functional theory (DFT). The electronic exchange-correlation potential is approached using the spin generalized gradient approximation (spin-GGA). The structural properties of the $Zn_{1-x}V_xTe$ alloys ($x=0$, 0.25, 0.50, 0.75 and 1) are given for the lattice constants and the bulk moduli and their pressure derivatives. The elastic constants C_{11}, C_{12} and C_{44} are calculated using numerical first-principles calculations implemented in the WIEN2k package. An analysis of the band structures and the densities of states reveals that $Zn_{0.50}V_{0.50}Te$ and $Zn_{0.75}V_{0.25}Te$ exhibit a half-metallic character, while $Zn_{0.25}V_{0.75}Te$ is nearly half-metallic. The band structure calculations are used to estimate the spin-polarized splitting energies $\Delta_x(d)$ and $\Delta_x(pd)$ produced by the V(3*d*)-doped and *s*(*p*)–*d* exchange constants $N_{0\alpha}$ (conduction band) and $N_{0\beta}$ (valence band). The *p*–*d* hybridization reduces the magnetic moment of V from its atomic charge value of $3\mu_B$ and creates small local magnetic moments on the nonmagnetic Zn and Te sites. Finally, we present the thermal effect on the macroscopic properties of these alloys, such as the thermal expansion coefficient, heat capacity and Debye temperature, based on the quasi-harmonic Debye model.

1. Introduction

ZnTe is an important II–VI semiconductor that crystallizes in the zinc blende structure and is an attractive material for the development of various recent technologies of solids in optical device applications, such as visual displays, high-density optical memories, photodetectors, transparent conductors and solar cells [1] and other photo-electronic devices such as high-efficiency thin film transistors and light-emitting diodes [2].

Half-metallic (HM) ferromagnetic and diluted magnetic semiconductors (DMS) of II–VI semiconductors being alloyed with transition metals such as V, Cr, Mn, Fe, Co and Ni have found wide applications in spintronics due to their potential application and their exceptional electronic structure [3,4], in which one of the two spin channels is metallic and the other is semiconducting or insulating with a spin-polarized energy gap at the Fermi level. A diluted magnetic semiconductor (DMS) applies when the fraction of the doped transition metal cations is very small. The first prediction was made by Groot et al. [5] for the half-Heusler alloys NiMnSb and PtMnSb. Since then, the half-metallic ferromagnets have seen a large evolution of theoretical and experimental applications in spintronics such as the metal oxides Fe_3O_4 [6] and CrO_2 [7,8], full-Heusler compounds Co_2MnSi [9] and Co_2FeSi [10], perovskite alloys $La_{0.7}Sr_{0.3}MnO_3$ [11] and Sr_2FeMoO_6 [12] and chalcogenides with the zinc blende structure [13]. Half-metallic ferromagnets have also been observed in transition-metal-doped semiconductors, such as $Zn_{1-x}Cr_xSe$ [14], $Al_{1-x}Cr_xAs$ [15], $Zn_{1-x}Cr_xS$, $Cd_{1-x}Cr_xS$ [16] and $Cd_{1-x}Cr_xTe$ [17] and in diluted magnetic semiconductors such as Cr-doped BeSe and BeTe [18,19], Mn-doped GaN and AlSb [20,21], Cr- and Mn-doped AlN, V- and Cr-doped GeTe and Mn and Cr-doped ZnTe [22–28]. There exists at

* Corresponding author Fax: +213 45802923;
E-mail address: khenata_rabah@yahoo.fr (R. Khenata).

http://dx.doi.org/10.1016/j.jmmm.2014.10.070
0304-8853/

least one experimental application by doping Mn and Cr in ZnTe [29,30].

The objective of the present work is to investigate the structural, elastic, electronic structure, magnetic and thermal properties of V-doped zinc blende ZnTe using the first-principles full potential linearized augmented plane wave (FP-LAPW) method within the generalized gradient approximation (PBE-GGA). We observed that for $x=0.50$, $Zn_{0.5}V_{0.5}Te$ has a half-metallic character, whereas for $x=0.25$ and 0.75, $Zn_{0.75}V_{0.25}Te$ and $Zn_{0.25}V_{0.75}Te$ are nearly half-metallic.

The remainder of the paper is organized as follows. Section 2 describes the calculation method. Section 3 presents the results and a discussion of the structural, elastic, electronic, magnetic and thermal properties, and finally, Section 4 summarizes the conclusions of this work.

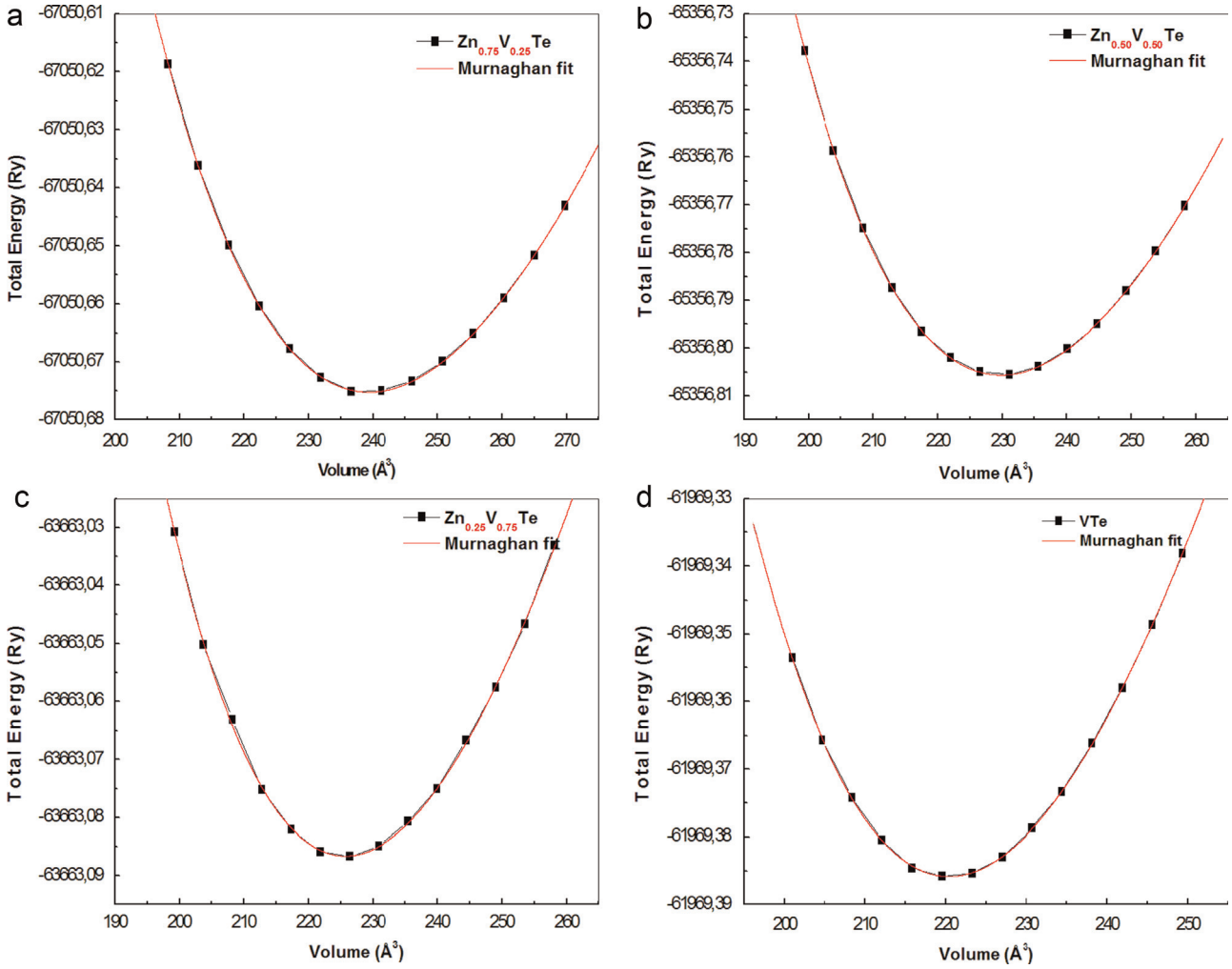

Fig. 1. Calculated total energy optimization variation versus volume for ZB $Zn_{1-x}V_xSe$ alloys at (a) $x=0.25$, (b) $x=0.50$, (c) $x=0.75$ and (d) $x=1$.

Table 1
Calculated equilibrium lattice constant a_0 and bulk modulus B and its pressure derivatives B' for $Zn_{1-x}V_xTe$ alloys.

Composition	Lattice parameter a_0 (Å)			Bulk modulus B (GPa)			B'		
x	This work	Cal.	Exp.	This work	Cal.	Exp.	This work	Cal.	Exp.
0.00	6.2208	6.029[b] 6.183[c]	6.089[a]	44.29	55.9 [b] 43.7 [c]	50.9[a]	4.78	5.1[b] 6.01[c]	5.04[a] –
0.25	6.2103	–	–	46.00	–	–	4.74	–	–
0.50	6.1256	–	–	55.09	–	–	4.85	–	–
0.75	6.0872	–	–	62.77	–	–	4.55	–	–
1.00	6.0403	6.223[d] 6.271[e]	–	68.90	– –	–	4.60	50.3[d]	–

[a] Ref. [53].
[b] Ref. [54].
[c] Ref. [55].
[d] Ref. [56].
[e] Ref. [57].

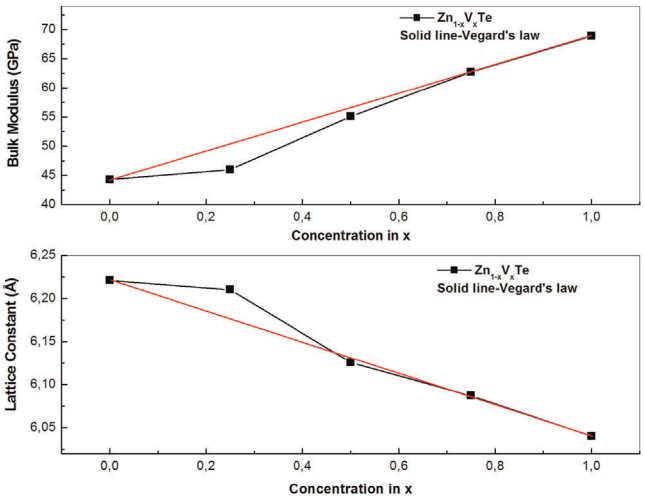

Fig. 2. Comparison between the lattice constant and bulk modulus for ZB $Zn_{1-x}V_xTe$ alloys using Vegard's law as a function of x.

2. Calculation method

The structural, elastic, electronic, magnetic and thermal properties of $Zn_{1-x}V_xTe$ (x=0, 0.25, 0.50, 0.75 and 1) were determined using the first-principles full potential linearized augmented plane wave method (FP-LAPW) as implemented in the WIEN2k package [31] within spin-polarized density functional theory (DFT) [32]. The spin-generalized gradient approximation (Spin-GGA) as parameterized by Perdew et al. [33] was used to describe the exchange-correlation potential. The atomic radius (muffin-tin R_{MT}) was chosen to be 2.34, 2.20 and 2.34 a.u. for Zn, Te and V, respectively. The Zn ($4s^2 3d^{10}$), Te ($5s^2 4d^{10} 5p^4$) and V ($4s^2 3d^3$) states were considered as valence electrons. The $R_{MT} \times K_{max}$ parameter was taken as 8 to determine the matrix size, where R_{MT} is the smallest muffin-tin (MT) sphere radius, and K_{max} is the maximum modulus for the reciprocal lattice vectors K. The integration in the Brillouin zone (BZ) was performed using 35 special k-points based on a mesh of $8 \times 8 \times 8$ in the first (BZ). The self-consistent iteration process was repeated until the total energy convergence was less than 10^{-4} Ry. The investigations of the thermal effects were performed using the quasi-harmonic Debye model implemented in the Gibbs program [34] to determine all the thermodynamic parameters as a function of temperature and pressure, which were used to determine other macroscopic properties [34–38].

The ZnTe compound has the zinc blende crystal structure (space group $F\bar{4}3$ m (No. 216)) with an experimental lattice constant of 6.089 Å [39]. The replacement of Zn atoms by V in ZnTe creates $Zn_{1-x}V_xTe$ alloys. For x=0.25 and 0.75, V atoms are located at the apex and the face-center sites of the cubic crystal with space group $P\bar{4}3$ m (No. 215), respectively. In the case of x=0.50, the V atoms occupy the four center sites of the unit cell, and thus the space group is transformed to $P\bar{4}$m2 (No. 115).

3. Results and discussion

3.1. Structural properties

The empirical Birch-Murnaghan equation of states [40] is employed to determine the equilibrium lattice parameters by minimizing the total energy depending on the volume of the $Zn_{1-x}V_xTe$ alloys (x=0, 0.25, 0.50, 0.75 and 1):

$$E(V) = a + bV^{-2/3} + cV^{-4/3} + dV^{-6/3}, \quad (1)$$

where V is the volume and a, b, c and d are fitting parameters. The equilibrium structural parameters consist of the lattice constant (a_0), the bulk modulus (B_0) and its pressure derivative (B') and the minimum energy (E_0). The ferromagnetic GGA-calculations of the optimized total energy versus the cell volume of the $Zn_{1-x}V_xTe$ alloys (x=0.25, 0.50, 0.75 and 1) in the B3 phase are shown in Fig. 1. Table 1 lists the values of the structural equilibrium parameters such as (a_0), (B_0) and (B'). We observe that for the binary ZnTe and VTe compounds, the equilibrium lattice parameters are in good agreement with other works available in the literature. The maximum deviations between these values of the lattice constants and the experimental/theoretical ones are 2.16% for ZnTe and 2.93% for VTe. For the ternary alloys $Zn_{1-x}V_xTe$, no experimental data or theoretical calculations are available in the literature. Fig. 2 shows the evolution of the lattice constant and the bulk modulus as a function of the V-doping concentration, where the lattice constant decreases and the bulk modulus increases with concentration (x) which proves that V-doping enhance the hardness of the crystal system.

3.2. Elastic properties

The calculations of the elastic moduli of the zinc blende $Zn_{1-x}V_xTe$ alloys for small strains are treated using the Charpin method that was recently developed and implemented in the WIEN2k code [31]. The elastic moduli are obtained from the generalized Hooke's law, which relates the strains (ε) to the stresses (σ) as follows:

$$\begin{bmatrix} \sigma 11 \\ \vdots \\ \sigma 61 \end{bmatrix} = \begin{bmatrix} c11 & \cdots & c16 \\ \vdots & \ddots & \vdots \\ c61 & \cdots & c66 \end{bmatrix} \times \begin{bmatrix} \varepsilon 11 \\ \vdots \\ \varepsilon 61 \end{bmatrix} \quad (2)$$

The independent elastic constants for the cubic system are (C_{11}, C_{12} and C_{44}).

Table 2
Calculated elastic constants C_{ij} (in GPa) for $Zn_{1-x}V_xTe$ alloys.

Composition	C_{11}			C_{12}			C_{44}		
x	This work	Cal.	Exp.	This work	Cal.	Exp.	This work	Cal.	Exp.
0.00	60.43	98[b]	71.7[a]	35.72	31.8[b]	40.7[a]	28.82	23.3[b]	31.2[a]
0.25	63.09	–	–	46.55	–	–	36.77	–	–
0.50	63.81	–	–	55.41	–	–	42.76	–	–
0.75	65.43	–	–	65.25	–	–	49.69	–	–
1.00	67.07	–	–	75.06	–	–	56.64	–	–

[a] Ref. [58].
[b] Ref. [59].

Table 3
Calculated anisotropy (A), Zener anisotropy ratio (A') and universal anisotropy (A^U) for $Zn_{1-x}V_xTe$ alloys.

Composition	A			A'			A^U		
x	This work	Cal.	Exp.	This work	Cal.	Exp.	This work	Cal.	Exp.
0.00	0.9785	−0.2[b]	0.439[a]	2.3325	0.704[b]	2.013[a]	0.9135	0.152[b]	1.716[a]
0.25	0.8859	–		4.3258	–	–	3.0683	–	–
0.50	1.2094	–	–	10.222	–	–	9.9842	–	–
0.75	1.5161	–	–	522.94	–	–	625.14	–	–
1.00	1.8008	–	–	−14.177	–	–	–	–	–

[a] Ref. [58].
[b] Ref. [59].

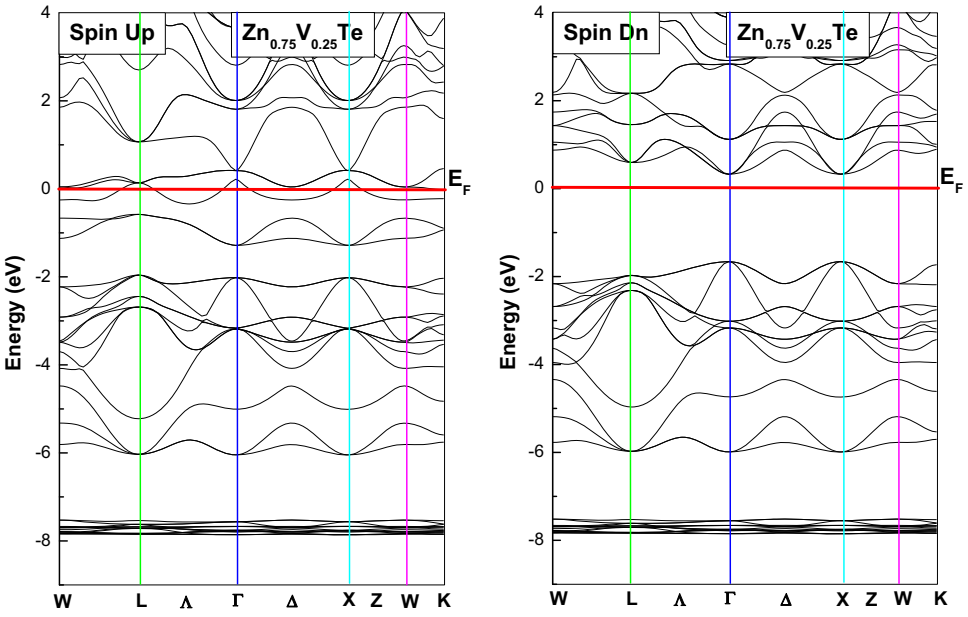

Fig. 3. Spin-polarized electronic band structure of ZB $Zn_{0.75}V_{0.25}Te$ at the equilibrium lattice parameter.

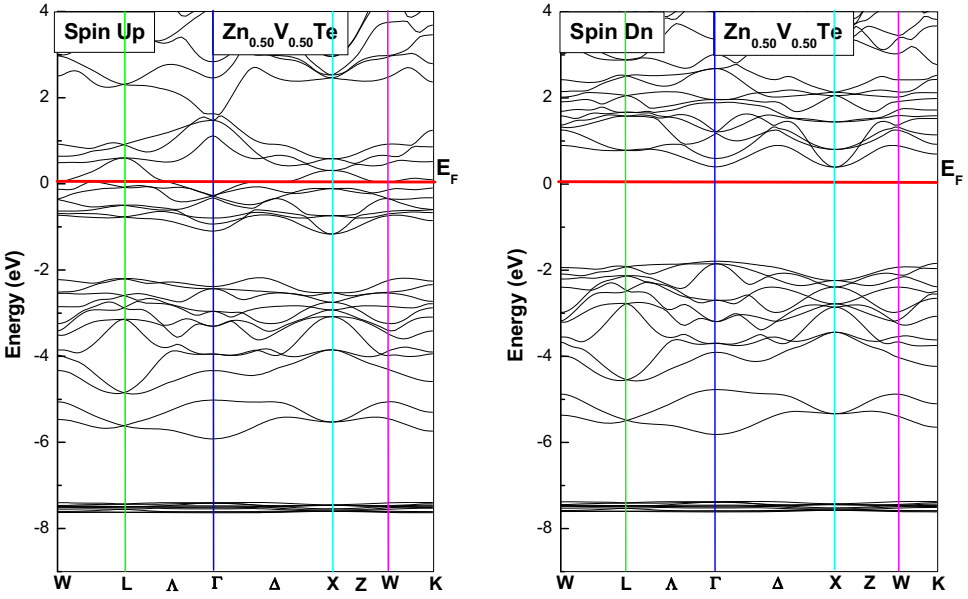

Fig. 4. Spin-polarized electronic band structure of ZB $Zn_{0.50}V_{0.50}Te$ at the equilibrium lattice parameter.

C_{11} and C_{12} are estimated by using the first equation of the bulk modulus

$$B = (C_{11} + 2C_{12})/3. \quad (3)$$

And the second equation involves the volume conservation of the tetragonal strain tensor

$$\begin{bmatrix} \delta & 0 & 0 \\ 0 & \delta & 0 \\ 0 & 0 & \dfrac{1}{(1+\delta)^2 - 1} \end{bmatrix}, \quad (4)$$

where the expression of the total energy is

$$E(\delta) = E(-\delta) = E(0) + 3(C_{11} - C_{12})V_0\delta^2 + O(\delta^3), \quad (5)$$

with V_0 representing the volume of the unit cell.

To determine C_{44}, we used the volume conservation of the monoclinic strain tensor:

$$\begin{bmatrix} 1 & \delta/2 & 0 \\ \delta/2 & 1 & 0 \\ 0 & 0 & 4/4 - \delta^2 \end{bmatrix}. \quad (6)$$

The total energy then becomes

$$E(\delta) = E(-\delta) = E(0) + \frac{C44}{4}V_0\delta^2 + O(\delta^3). \quad (7)$$

The mechanical stability of a cubic crystal is defined by satisfying the Born stability criteria [41]

$$C_{44} > 0 \quad (8a)$$

$$C_{11} - |C_{12}| > 0 \quad (8b)$$

$$C_{11} + 2C_{12} > 0. \quad (8c)$$

Table 2 presents the calculated C_{11}, C_{12} and C_{44} for the $Zn_{1-x}V_xTe$ alloys at $x=0$, 0.25, 0.50, 0.75, and 1, compared with the available experimental data. The estimated maximum error of this work is no larger than 38.34%. The C_{12} and C_{44} elastic constants of the binary ZnTe and VTe compounds are in good agreement with other experimental and theoretical data; however, for C_{11} the difference to the values available in the literature is large. For the ternary $Zn_{1-x}V_xTe$ alloys, the present work acts as a good reference for further works. According to the Born stability criteria, the $Zn_{1-x}V_xTe$ compounds are mechanically stable.

The elastic anisotropy is an important parameter to understand the thermal expansion properties and demonstrate the durability of the compound [42], which is defined as $A=(2C_{44} - (C_{11}-C_{12}))/C_{11}$ [43]. Thus, we estimate the universal elastic anisotropy for the cubic system defined by Ranganathan and Ostoja-Starzewski [44]: $A^U = 6/5 \times (\sqrt{A'} - 1/\sqrt{A'})^2$, where A' is the Zener anisotropy ratio, which is defined as $A'=2C_{44}/(C_{11}-C_{12})$. Table 3 summarizes the values of A, A' and A^U for the $Zn_{1-x}V_xTe$ alloys; these alloys are not anisotropic compounds.

3.3. Electronic properties

3.3.1. Spin-polarized band structure energies

The spin-polarized band structure energies of ternary $Zn_{1-x}V_xTe$ alloys for $x=0.25$, 0.50 and 0.75 were calculated using the PBE-GGA scheme at their equilibrium lattice parameters, as listed in Table 1. The majority and minority spin (spin-up and spin-down) band structures along the high symmetry directions of the first Brillouin zone are depicted in Figs. 3–5 for $Zn_{0.75}V_{0.25}Te$, $Zn_{0.50}V_{0.50}Te$ and $Zn_{0.25}V_{0.75}Te$, respectively, where the bottom of the conduction band and the top of the valence band are at the point Γ. According to Figs. 3 and 4 for the $Zn_{0.75}V_{0.25}Te$ and $Zn_{0.50}V_{0.50}Te$, in the spin-up case, the energy bands cross the Fermi level, whereas for the spin-down case the Fermi level lies in the

Table 4
Calculated results of the half-metallic E_{HM} (eV) band gaps and spin-minority band gaps E_g (eV) of each site in $Zn_{1-x}V_xTe$ alloys.

Alloy	Composition	E_g			*EHM*		
	x	This work	Cal.	Exp.	This work	Cal.	Exp.
$Zn_{0.75}V_{0.25}Te$	0.25	1.96	–	–	0.34	–	–
$Zn_{0.50}V_{0.50}Te$	0.50	2.04	–	–	0.30	–	–
$Zn_{0.25}V_{0.75}Te$	0.75	1.96	–	–	–	–	–
VTe	1.00	2.74	2.80[a]	–	0.05[a]	–	–

[a] Ref. [60].

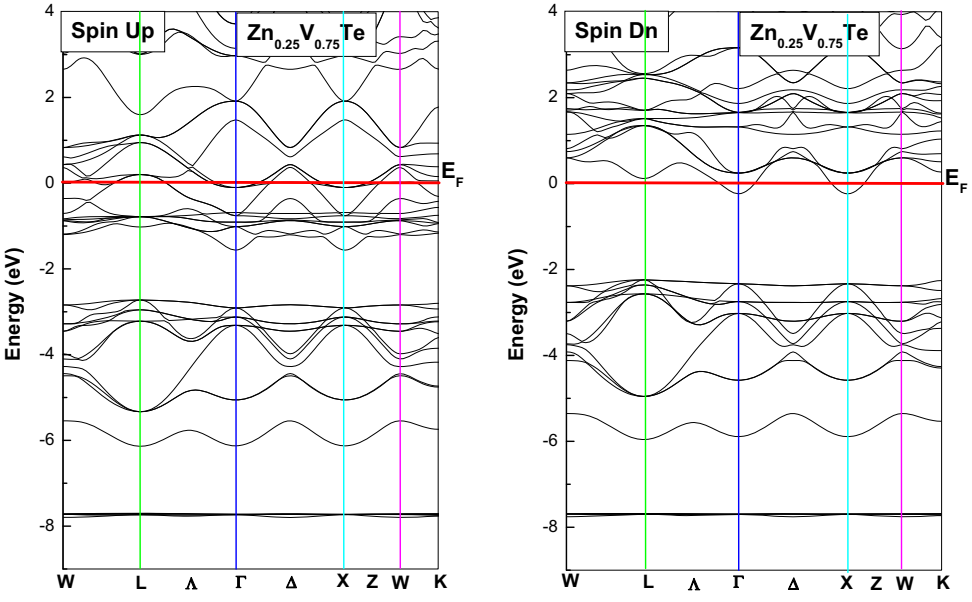

Fig. 5. Spin-polarized electronic band structure of ZB $Zn_{0.25}V_{0.75}Te$ at the equilibrium lattice parameter.

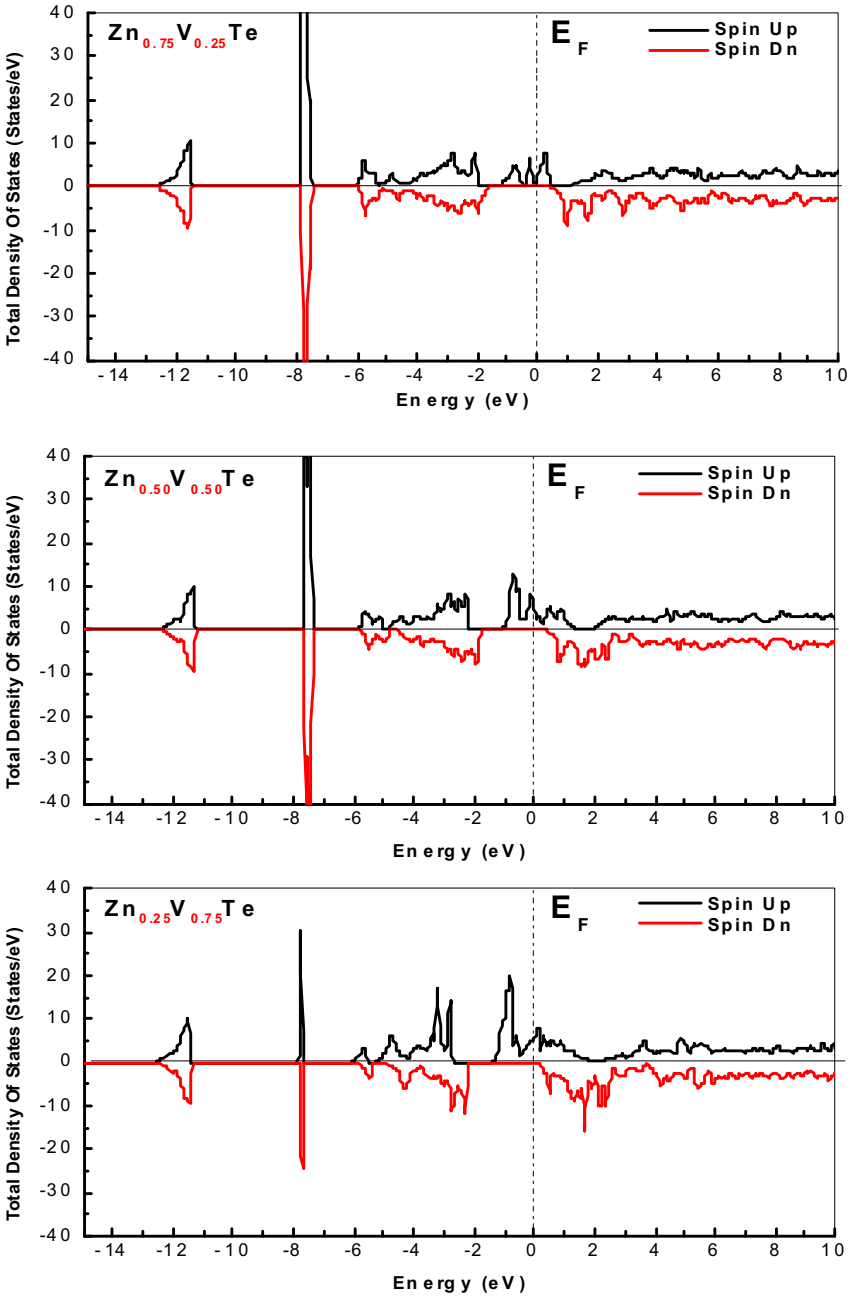

Fig. 6. Spin-dependent total density of states (TDOS) for ZB $Zn_{1-x}V_xTe$ alloys (x=0.25, 0.50 and 0.75).

gap which confirms the half-metallic nature of these alloys. Fig. 5 shows the band structure of the $Zn_{0.25}V_{0.75}Te$ alloy; one energy band crosses the Fermi level for the spin-down case that demonstrates that this compound has a nearly half-metallic character. The half-metallic energy gap is defined as the maximum between the lowest energy of the spin-up and spin-down conduction bands with respect to the Fermi level and the absolute values of the highest energy of the spin-up and spin-down valence bands [45,46]. Table 4 presents the values of the spin-down energy gap (E_g) and the half-metallic energy gap (E_{HM}) of the $Zn_{0.75}V_{0.25}Te$ and $Zn_{0.50}V_{0.50}Te$ alloys obtained using the PBE-GGA approximation. One can remark that (E_{HM}) increases with the concentration of x from 0.25 to 0.50, but then decreases at x=0.75. The wider (E_{HM}) gaps at x=0.25 and 0.50 predict that high Curie temperature can be expected in these materials [47].

3.3.2. *Density of states*

The electronic properties of solids were investigated in further detail using the useful quantity of the electronic density of states. The calculations of the total and partial density of states (TDOS and PDOS, respectively) plots of the $Zn_{1-x}V_xTe$ alloys (x=0.25, 0.50 and 0.75) in the ferromagnetic phase at their equilibrium lattice parameters are presented in Figs. 6 and 7 for spin-up and spin-down channels, respectively. Near the Fermi level, the alloys exhibit a large exchange splitting between the majority and minority spin states. Fig. 6(a) and (b) indicate that the majority spin electrons have a metallic nature for both the $Zn_{0.75}V_{0.25}Te$ and $Zn_{0.50}V_{0.50}Te$ alloys, whereas a band gap appears around the Fermi level for the minority spin states which exhibit a semiconducting behavior. Therefore, $Zn_{0.75}V_{0.25}Te$ and $Zn_{0.50}V_{0.50}Te$ are half-metallic ferromagnetic compounds. The TDOS of $Zn_{0.25}V_{0.75}Te$ is shown in Fig. 6(c) with only one energy band crossing the Fermi

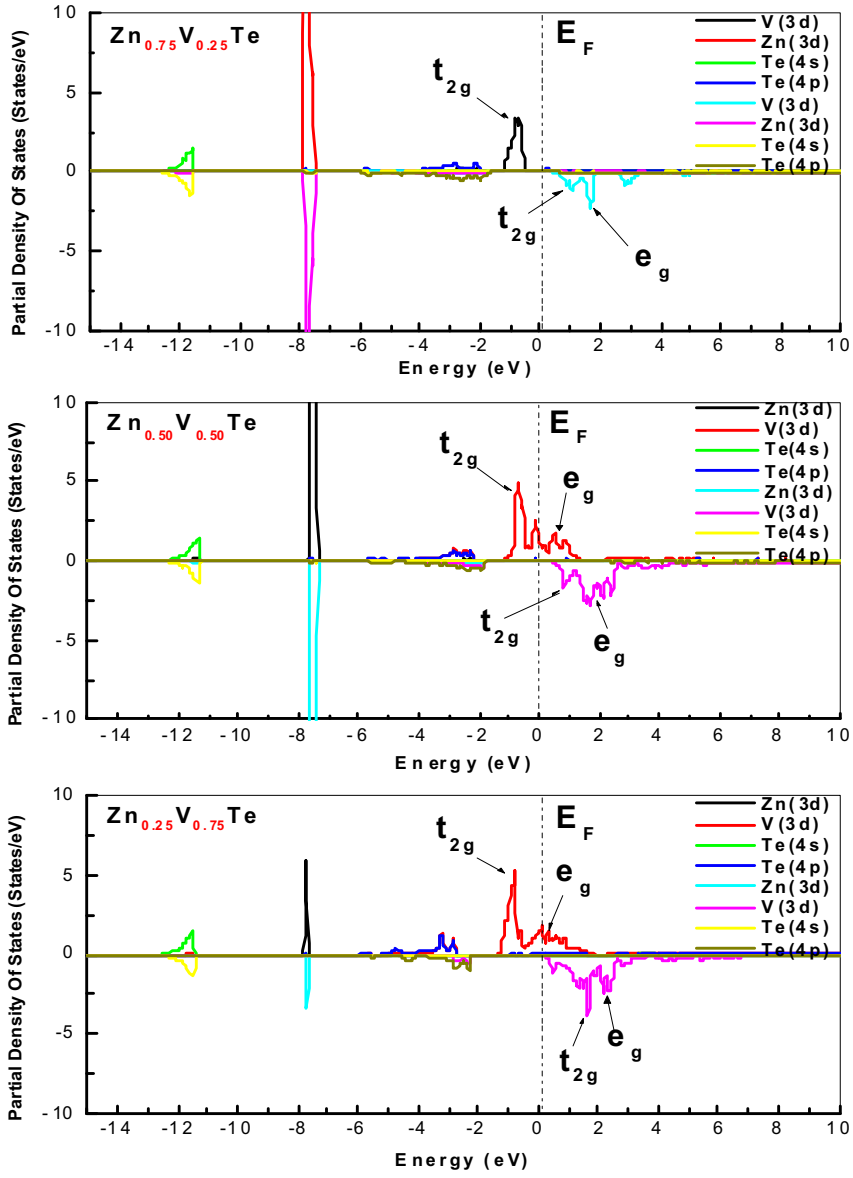

Fig. 7. Spin-dependent partial density of states (PDOS) for ZB $Zn_{1-x}V_xTe$ alloys (x=0.25, 0.50 and 0.75).

Table 5
Calculated conduction and valance band-edge spin-splitting $\Delta_x(d)$ and $\Delta_x(pd)$ and exchange constants of $Zn_{1-x}V_xTe$ alloys for (a) x=0.25, (b) x=0.50 and (c) x=0.75.

Alloy	x	$\Delta_x(d)$	$\Delta_x(pd)$	$N_0\alpha$	$N_0\beta$
$Zn_{1-x}V_xTe$	0.25	1.442	−1.618	0.682	−3.236
	0.50	2.394	−1.738	0.322	−1.738
	0.75	2.449	−2.171	−0.141	−1.447

Table 6
Calculated results of the total magnetic moment (M_{tot} in μ_B) per formula unit and local magnetic moments for each concentration for $Zn_{1-x}V_xTe$ alloys.

Alloy	$Zn_{0.75}V_{0.25}Te$	$Zn_{0.50}V_{0.50}Te$	$Zn_{0.25}V_{0.75}Te$	VTe
M_{Tot}	3.005	3.000	2.991	2.544
M_V	2.518	2.532	2.291	2.254
M_{Zn}	0.043	0.065	0.075	–
M_{Te}	−0.033	−0.045	−0.039	−0.063

level making this compound nearly half-metallic. From the PDOS, we observe for all three compounds that the energy bands around -7.75 eV are mainly arising from the Zn d states. In the energy range from −6.20 eV to −1.61 eV the DOS comes from the Te p states with small contributions of V 3d, Zn s and p states. Near the Fermi level, an important hybridization between Se 4p and V 3d states occurs. The majority spin part between −1.29 eV and −0.43 eV originates from V t_{2g} states with a small contribution of V e_g states, which is responsible for the strong V t_{2g}-Te p hybridization and weak V e_g-Te p hybridization.

For the V 3d states, the $\Delta_x(d)$ exchange splitting is defined as the difference between the peaks on DOS of the majority-spin and minority-spin. The $\Delta_x(d)$ of all alloys is listed in Table 5. To describe the nature of the attraction, we calculate the p-d exchange splitting $\Delta_x(pd)$

$$\Delta_x(pd) = E_v(\downarrow) - E_v(\uparrow), \tag{9}$$

where $E_v(\downarrow)$ and $E_v(\uparrow)$ are the valence band maxima of the minority spin and majority spin, respectively. The values of $\Delta_x(pd)$

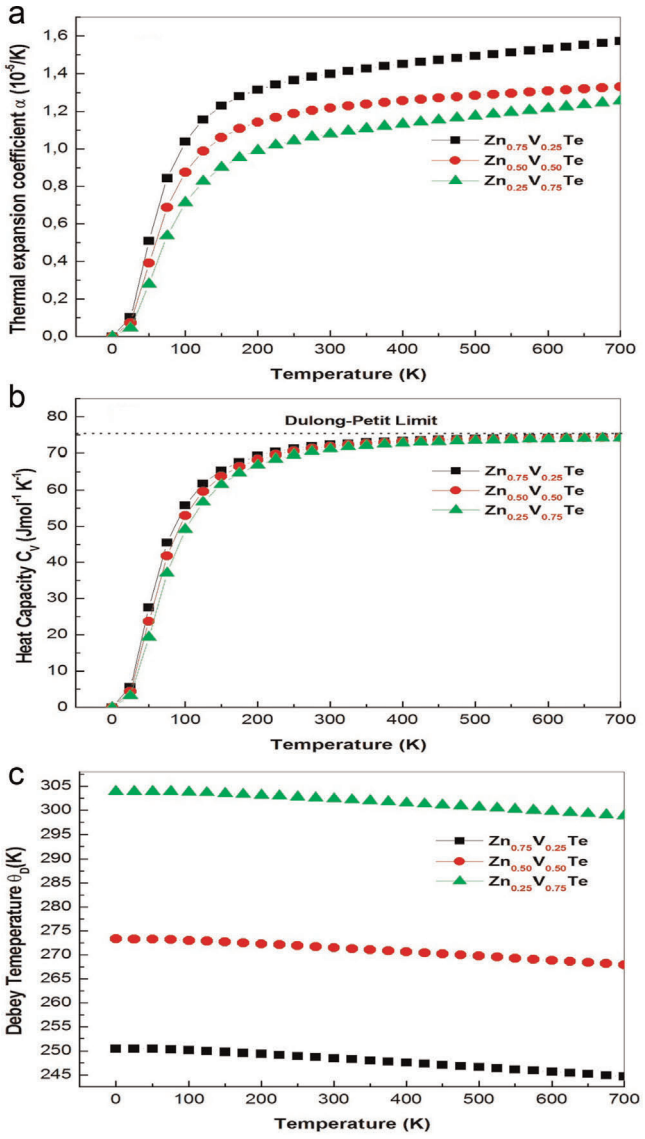

Fig. 8. The variation of the thermal expansion α (a), heat capacity C_v (b) and Debye temperature θ_D (c), versus temperature at zero pressure for ZB $Zn_{1-x}V_xTe$ alloys (x=0.25, 0.50 and 0.75).

are negative, confirming that the effective potential is more attractive for the minority spin than for the majority spin [48].

3.4. Magnetic properties

3.4.1. Exchange coupling

Using the spin-polarized electronic structure of the zinc blende $Zn_{1-x}V_xTe$ alloys in the ferromagnetic states we can estimate two important parameters namely the s–d exchange constant $N_0\alpha$ (conduction band) and the p–d exchange constant $N_0\beta$ (valence band), where N_0 corresponds to the cation concentration. Assuming the usual Kondo interaction, $N_0\alpha$ and $N_0\beta$ can be defined as [49]

$$N_0\alpha = \frac{\Delta E_c}{x(S)};\ N_0\beta = \frac{\Delta E_v}{x(S)}, \tag{10}$$

where ΔE_c and ΔE_v are the conduction and the valence edge splitting at the Γ- point and x is the concentration of V and (S) denotes the average magnetization of the V atoms. The obtained values are summarized in Table 5 and show that $N_0\alpha$ has a negative sign, while $N_0\beta$ is positive, which confirms that the valence and the conduction states exhibit opposite behavior according the exchange splitting. Additionally, we indicate that the decrease of $N_0\alpha$ with increasing V concentration is due to the number of V 3d states being more than that of Te 5p states.

3.4.2. Magnetic moment

Using the PBE-GGA, we calculated the total magnetic moments (M_{Tot}) of the zinc blende $Zn_{1-x}V_xTe$ alloys (x=0.25, 0.50, 0.75 and 1) and the atomic magnetic moments of Zn, V and Te, which are presented in Table 6. The values of M_{Tot} show that the main contribution is due to the V atom with small contributions originating from the Zn and Te atoms, which exhibits the half-metallic nature of the compounds. We can also see that the atomic magnetic moments of V and Te have opposite signs due to the antiferromagnetic interaction between the Te and V valence spins. Such a behavior was also reported by Ge and Zhang [50]. According to Table 6, the p–d hybridization near the Fermi level decreases the atomic magnetic moment of the V atom from its atomic charge value of 3μ_B and creates small local magnetic moments on the nonmagnetic Zn and Te sites.

3.5. Thermal properties

To study the thermal effects on certain physical properties in the crystal, such as the thermal expansion coefficient, specific heat at constant volume C_v and constant pressure C_p and Debye temperature, we used the Gibbs code based on the quasi-harmonic Debye model [34].

The calculated thermal expansion coefficient (α) as a function of temperature at zero pressure is displayed in Fig. 8(a), where we observe that the thermal expansion coefficient for all the compounds increases sharply with the increase of temperature up to 100 K. Above 100 K, we observe a weak increase towards a constant value. The thermal expansion coefficient of the $Zn_{0.75}V_{0.25}Te$, $Zn_{0.50}V_{0.50}Te$, $Zn_{0.25}V_{0.75}Te$ alloys (at room temperature and zero pressure) are 4.09×10^5, 3.38×10^5 and 3.24×10^5 K^{-1}, respectively.

The variation of the specific heat at constant volume C_v versus temperature at zero pressure of the alloys is shown in Fig. 8(b). At low temperature, c_v increases as T^3 [51], whereas at high temperature, c_v increases slowly to tend the Petit and Dulong limit [52]. At room temperature and zero pressure, the c_v values of the $Zn_{0.75}V_{0.25}Te$, $Zn_{0.50}V_{0.50}Te$, $Zn_{0.25}V_{0.75}Te$ compounds are 187.48 J mol^{-1} K^{-1}, 185.19 J mol^{-1} K^{-1} and 181.93 J mol^{-1} K^{-1}, respectively.

The Debye temperature (θ_D) is an important parameter characteristic for the thermal properties of solids. It is the temperature above which the crystal behaves classically, because the thermal vibrations become more important than the quantum effects. Fig. 8(c) shows the evolution of θ_D with temperature. It can be seen that θ_D is nearly constant from 0 to 100 K and for T ≥ 100 K, θ_D decreases linearly with increasing temperature. The calculated Debye temperatures (θ_Ds) of the $Zn_{0.75}V_{0.25}Te$, $Zn_{0.50}V_{0.50}Te$, $Zn_{0.25}V_{0.75}Te$ alloys at room temperature and zero pressure are 337.23 K, 369.56 K and 411.98 K, respectively.

4. Conclusions

We have investigated the structural, elastic, electronic, magnetic and thermal properties of $Zn_{1-x}V_xTe$ alloys (x=0.25, 0.50 and 0.75) in the B3 phase by employing the FP-LAPW approach within DFT. Our predictions at the equilibrium lattice parameters reveal that the $Zn_{0.75}V_{0.25}Te$ and $Zn_{0.50}V_{0.50}Te$ alloys are half-metallic ferromagnetic compounds, whereas the $Zn_{0.25}V_{0.75}Te$ alloy is nearly half-metallic since only one band crossed the Fermi level near the Γ point. The elastic properties of the ternary $Zn_{1-x}V_xTe$ alloys are calculated for the first time and should be used as a

reference for future similar projects. The V 3*d* states cause the exchange splitting $\Delta_x(d)$ and $\Delta_x(pd)$ parameters, which are derived from TDOS and PDOS plots. The negative values of $\Delta_x(pd)$ explain that the effective potential of the minority spin, which is more attractive than that of the majority spin. The exchange constants $N_0\alpha$ and $N_0\beta$ were estimated and have values of opposite sign, which confirms that the valence and conduction states interact in an opposite manner during the exchange-splitting process. Due to the strong hybridization between the V t_2g and Te 5*p* states, the atomic magnetic moment of the V atom is reduced from its atomic charge of $3\mu_B$, and small local magnetic moments are generated on the nonmagnetic Zn and Te sites. Using the quasi-harmonic Debye model, the thermal expansion coefficient, lattice heat capacity and Debye temperature versus temperature were investigated in detail.

Acknowledgments

The authors (Khenata and Bin Omran) acknowledge support by the National Plan for Science, Technology and Innovation under the research project No. ADV-1498. Y.A. would like to acknowledge the University Malaysia Perlis for Grant No. 9007-00062 and TWAS-Italy for the full support of his visit to JUST-Jordan under the TWAS-UNESCO Associateship. The authors (Bouhemadou, Bin-Omran and Khenata) extend their appreciation to the Deanship of Scientific Research at King Saud University for funding the work through research group project No RGP-VPP-088.

References

[1] S. Zh Karazhanov, P. Ravindran, A. Kjekshus, H. Fjellvag, B.G. Svensson, Phys. Rev. B 75 (2007) 155104.
[2] K. Sato, M. Hanafusa, A. Noda, A. Arakawa, M. Uchida, T. Asahi, O. Oda, J. Cryst. Growth 214/215 (2000) 1080.
[3] G.A. Prinz, Science 282 (1998) 1660.
[4] S.A. Wolf, D.D. Awschalom, R.A. Buhrman, J.M. Daughton, S. von Molnar, M. L. Roukes, A.Y. Chtchelkanova, D.M. Treger, Science 294 (2001) 1488.
[5] R.A. de Groot, F.M. Mueller, P.G. van Engen, K.H.J. Buschow, Phys. Rev. Lett. 50 (1983) 2024.
[6] F.J. Jedema, A.T. Filip, B.V. Wees, Nature 410 (2001) 345.
[7] N.E. Brener, J.M. Tyler, J. Callaway, D. Bagayoko, G.L. Zhao, Phys. Rev. B 61 (2000) 16582.
[8] K. Schwarz, J. Phys. F: Met. Phys. 16 (1986) L211.
[9] I. Galanakis, Phys. Rev. B 71 (2005) 012413.
[10] S. Wurmehl, G.H. Fecher, H.C. Kandpal, V. Ksenofontov, C. Felser, H. Lin, Appl. Phys. Lett. 88 (2006) 032503.
[11] R.J. Soulen Jr., J.M. Byers, M.S. Osofsky, B. Nadgorny, T. Ambrose, A. Barry, J.M. D. Coey, Science 282 (1998) 85.
[12] K.L. Kobayashi, T. Kimura, H. Sawada, K. Terakuraand, Y. Tokura, Nature 395 (1998) 677.
[13] M. Nakao, Phys. Rev. B 69 (2004) 214429.
[14] X.-F. Ge, Y.-M. Zhang, J. Magn. Magn. Mater. 321 (2009) 198.
[15] Y.-H. Zhao, G.-P. Zhao, Phys. Rev. B 80 (2009) 224417.
[16] S. Nazir, N. Ikram, S.A. Siddiqi, Y. Saeed, A. Shaukat, A.H. Reshak, Curr. Opin. Solid State Mater. Sci. 14 (2010) 1.
[17] N.A. Noor, S. Ali, A. Shaukat, J. Phys. Chem. Solids 72 (2011) 836.
[18] S. Picozzi, T. Shishidou, A.J. Freeman, B. Delly, Phys. Rev. B67 (2003) 165203.
[19] S.M. Alay-e-Abbas, K.M. Wong, N.A. Noor, A. Shaukat, Yong Lei, Solid State Sci. 14 (2012) 1525.
[20] T. Jungwirth, J. Sinova, J. Mašek, J. Kučera, A.H. Mac Donald, Rev. Mod. Phys. 78 (2006) 809.
[21] G. Rahman, S. Cho, S.C. Hong, Phys. Status Solidi B12 (2007) 4435.
[22] L.-J. Shi, B.-G. Liu, Phys. Rev. B 76 (2007) 115201.
[23] Y.-H. Zhao, W.-H. Xie, L.-F. Zhu, B.-G. Liu, J. Phys.: Condens. Matter 18 (2006) 10259.
[24] W.-H. Xie, B.-G. Liu, J. Appl. Phys. 96 (2004) 3559.
[25] Y. Liu, B.-G. Liu, J. Phys. D: Appl. Phys. 40 (2007) 6791.
[26] T.M. Giebultowicz, et al., Phys. Rev. B 48 (1993) 12817.
[27] H. Saito, V. Zayets, S. Yamagata, K. Ando, Phys. Rev. Lett. 90 (2003) 207202.
[28] M.G. Sreenivasan, J.F. Bi, K.L. Teo, T. Liew, J. Appl. Phys. 103 (2008) 043908.
[29] T.M. Giebultowicz, P. Klosowski, N. Samarth, J.K. Furdyna, Phys. Rev. B48 (1993) 12817.
[30] H. Saito, V. Zayets, S. Yamagata, K. Ando, Phys. Rev. Lett. 90 (2003) 207202.
[31] P. Blaha, K. Schwarz, P. Sorantin, S.K. Trickey, Comput. Phys. Commun. 59 (1990) 339.
[32] P. Hohenberg, W. Kohn, Phys. Rev. 136 (1964) B864.
[33] J.P. Perdew, S. Burke, M. Ernzerhof, Phys. Rev. Lett. 77 (1996) 3865.
[34] M.A. Blanco, E. Francisco, V. Luaña, Comput. Phys. Commun. 158 (2004) 57.
[35] M.A. Blanco, A. Martín Pendás, E. Francisco, J.M. Recio, R. Franco, J. Mol. Struct. Theochem. 368 (1996) 245.
[36] M. Flórez, J.M. Recio, E. Francisco, M.A. Blanco, A. Martín Pendás, Phys. Rev. B 66 (2002) 144112.
[37] E. Francisco, J.M. Recio, M.A. Blanco, A. Martín Pendás, J. Phys. Chem. 102 (1998) 1595.
[38] E. Francisco, M.A. Blanco, G. Sanjurjo, Phys. Rev. B 63 (2001) 094107.
[39] R.W.G. Wyckoff, 2nd ed.,Crystal Structures, 1, Wiley, New York (1986) 112.
[40] F.D. Murnaghan, Proc. Natl. Acad. Sci. USA 30 (1944) 5390.
[41] J.F. Nye, Physical Properties of Crystals: Their Representation by Tensors and Matrices, Oxford University Press, Oxford, 1985.
[42] P. Ravindran, L. Fast, P.A. Korzhavyi, B. Johansson, J. Wills, O. Eriksson, J. Appl. Phys. 84 (1998) 4891.
[43] B.B. Karki, L. Stixture, S.J. Clark, M.C. Warren, G.G. Ackland, J. Grain, Am. Mineral. 82 (1997) 51.
[44] S.I. Ranganathan, M. Ostoja-Starzewski, Phys. Rev. Lett. 101 (2008) 055504.
[45] K.L. Yao, G.Y. Gao, Z.L. Liu, L. Zhu, Solid State Commun. 133 (2005) 301.
[46] G.Y. Gao, K.L. Yao, E. Sasioglu, L.M. Sandratskii, Z.L. Liu, J.L. Jiang, Phys. Rev. B 75 (2007) 174442.
[47] J. Kübler, Phys. Rev. B 67 (2003) 220403R.
[48] V.L. Moruzzi, J.F. Janak, A.R. Williams, Calculated Electronic Properties of Metals, Pergamon, NewYork, 1978.
[49] J.A. Gaj, R. Planel, G. Fishman, Solid State Commun. 29 (1984) 861.
[50] X.-F. Ge, Y.-M. Zhang, J. Magn. Magn. Mater. 321 (2009) 198.
[51] P. Debye, Ann. Phys. 39 (1912) 789.
[52] A.T. Petit, P.L. Dulong, Ann. Chim. Phys. 10 (1819) 395.
[53] O. Madelung (Ed.), Numerical Data and Functional Relationships in Science and Technology, vol. 17, Landolt-Bornstein, New Series, Group III, Springer-Verlag, Berlin, 1987 (Parts a and b, 1982; vol. 22, Parta).
[54] S.H. Wei, A. Zunger, Phys. Rev. B 60 (1999) 5404.
[55] N.E. Christensen, O.B. Christensen, Phys. Rev. B 33 (1986) 4739.
[56] D. Huang, Y.J. Zhao, L.J. Chen, D.H. Chen, Y.Z. Shao, J. Appl. Phys. 104 (2004) 053709.
[57] W.-H. Xie, Y.- QXu, B.-G. Liu, D.G. Pettifor, Phys. Rev. Let. 91 (2003) 037204.
[58] B.H. Lee, J. Appl. Phys. 41 (1970) 2988.
[59] S.-G. Shen, J. Phys.: Condens. Matter 6 (1994) 8733.
[60] M. Sajjad, H.X. Zhang, N.A. Noor, S.M. Alay-e-Abbas, A. Shaukat, Q. Mahmood, J. Magn. Magn. Mater. 343 (2013) 177.